What a difference a methyl group makes – the selectivity of monoamine oxidase B towards histamine and *N*-methylhistamine

Aleksandra Maršavelski[a] and Robert Vianello*[a]

Abstract: Monoamine oxidase (MAO) enzymes catalyze the degradation of a very broad range of biogenic and dietary amines including many neurotransmitters in the brain, whose imbalance is extensively linked with the biochemical pathology of various neurological disorders. Although sharing around 70% sequence identity, both MAO A and B isoforms differ in substrate affinities and inhibitor sensitivities. Inhibitors that act on MAO A are used to treat depression, due to their ability to raise serotonin concentrations, while MAO B inhibitors decrease dopamine degradation and improve motor control in patients with Parkinson disease. Despite this functional importance, the contributions affecting MAO selectivity are poorly understood. Here we used a combination of MD simulations, MM–PBSA binding free energy evaluations, and QM cluster calculations to address the unexpected, yet challenging MAO B selectivity for *N*-methylhistamine (**NMH**) over histamine (**HIS**), differing only in a single methyl group distant from the reactive ethylamino centre. We show that a dominant selectivity contribution is offered by a lower activation free energy for **NMH** by 2.6 kcal mol^{-1}, in excellent agreement with the experimental $\Delta\Delta G^{\ddagger}_{EXP}$ = 1.4 kcal mol^{-1}, together with a more favourable reaction exergonicity and active site binding. This study also confirms the hydrophobic nature of the MAO B active site and underlines the important role of Ile199, Leu171 and Leu328 in properly orienting substrates for the reaction.

Introduction

Histamine (**HIS**) is an important mediator of many biological processes including inflammation, gastric acid secretion, neuromodulation, and regulation of immune function. It is formed by decarboxylation of the amino acid *L*-histidine in a reaction catalyzed by the histidine decarboxylase, and by microbiological action in the course of food processing, thus making it present in substantial amounts in many fermented foodstuffs and beverages, such as aged cheese, red wine, and sauerkraut. Due to its potent pharmacological activity even at very low concentrations, the synthesis, transport, storage, release and degradation of histamine have to be carefully regulated to avoid adverse reactions, since it can even be toxic when it is present either in excess or in the wrong metabolic context.[1] Histamine exhibits its diverse biological actions by binding to and thereby activating four different G-protein coupled receptors located at the surface of histamine responsive cells. The primary goal of histamine inactivation is its conversion to metabolites that will not activate histamine receptors, and this is achieved either by the methylation of the imidazole ring, catalyzed by histamine *N*-methyltransferase (HMT), or by the oxidative deamination of the primary amino group, catalyzed by diamine oxidase (DAO) (Scheme 1).[2]

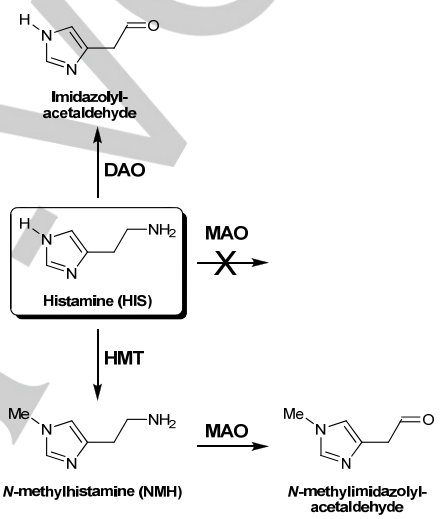

Scheme 1. Metabolic degradation of histamine (**HIS**) to the corresponding aldehyde directly catalyzed by diamine oxidase (DAO), or by monoamine oxidase (MAO) but only after **HIS** is converted to *N*-methylhistamine (**NMH**) with histamine methyltransferase (HMT).

HMT catalyzes the transfer of a methyl group from S-adenosyl-*L*-methionine to the secondary imidazole amino group forming *N*-methylhistamine (**NMH**), and is a highly specific enzyme that does not show significant methylation of other substrates. **NMH** is not active at the histamine receptor sites, and is further metabolized by monoamine oxidase (MAO), a primary degradation enzyme for a very broad range of structurally and chemically different biogenic and dietary amines in cells,[3] including amine neurotransmitters in the brain, which is why it has been the central pharmacological target for treating depression and Parkinson's disease for over 60 years.[4]

MAO is a mitochondrial outer membrane-bound flavoenzyme that catalyzes the oxidative deamination of amines into their corresponding imines, which are then non-enzymatically hydrolyzed to the final carbonyl compounds and ammonia. The enzyme itself is regenerated to its active form by molecular oxygen, O_2, which is in turn reduced to hydrogen peroxide, H_2O_2, according to the overall equation:

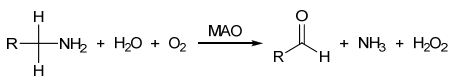

[a] Aleksandra Maršavelski, Dr. Robert Vianello*
Computational Organic Chemistry and Biochemistry Group, Ruđer Bošković Institute, Bijenička cesta 54, HR–10000 Zagreb, Croatia
E-mail: robert.vianello@irb.hr

Supporting information for this article is given via a link at the end of the document.((Please delete this text if not appropriate))

MAOs operate using the flavin adenine dinucleotide (FAD) cofactor, which is, in contrast to the majority of other flavoenzymes, covalently bound to a cysteine through an 8α-thioether linkage (Figure 1). During the catalytic reaction, FAD is reduced to $FADH_2$ by accepting two protons and two electrons from the substrate. Although having around 70% sequence identities and a conserved pentapeptidic sequence (Ser-Gly-Gly-Cys-Tyr) that binds the identical FAD cofactor,[5] both the A and the B isoforms of the enzyme differ on the basis of their substrate affinities and inhibitor sensitivities,[6] but it is assumed they act by the same mechanism. Each isoform is present in specific subsets of neurons, where they metabolize neurotransmitters, and both are found in liver, where biogenic amines are rapidly metabolized to less bioactive forms for excretion. Inhibition of MAOs has a notable neuroprotective effect, since the MAO catalyzed reactions yield neurotoxic products such as hydrogen peroxide and aldehydes.[7,8] However, despite tremendous research efforts devoted to MAOs over several decades, neither the catalytic nor the inhibition mechanisms of MAO have yet been unambiguously established.

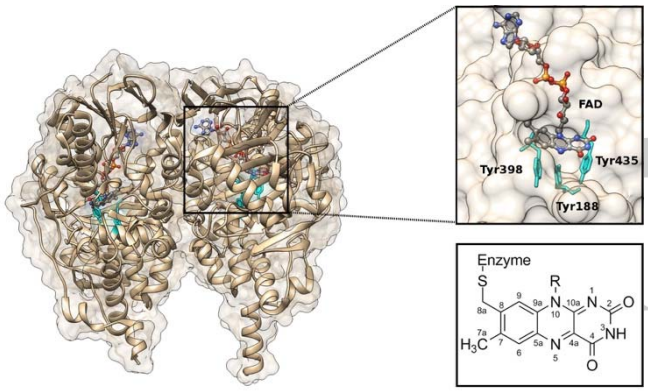

Figure 1. Position of the active site within the MAO B crystal structure (2XFN.pdb) indicating the flavin cofactor (FAD) and three tyrosine residues that all form the "aromatic cage" structural feature. Atom numbering of the FAD fragment is shown in the bottom-right box.

Recently, we performed the first quantum mechanical study that demonstrated the prevailing feasibility of the two-step direct hydride transfer mechanism over several alternative pathways for the dopamine degradation using QM-only cluster model of the MAO B enzyme.[9] This study was later extended by considering the full enzyme dimensionality through the empirical valence bond QM/MM approach, which gave the activation free energy of 16.1 kcal mol^{-1},[10] being in excellent agreement with the experimentally determined value of 16.5 kcal mol^{-1},[11] thus supporting the proposed hydride transfer mechanism. Our mechanistic picture is already gaining some affirmation in the literature,[12] and is fully corroborated by a very recent ^{13}C kinetic isotope effect measurements on a related polyamine oxidase flavoenzyme.[13] The focus of the present work will be on employing this mechanism in understanding differences in **HIS** and **NMH** degradation.

After successful heterologous over-expression and purification of recombinant human MAO in yeast,[14] the three-dimensional structures of human MAO A and MAO B have been solved at a resolution of 2.2 Å and 1.65 Å, respectively.[15,16] These showed that the active-site cavities are reached from the flavin-binding site at the core to the surface of the protein and are mainly hydrophobic, ending in an "aromatic cage" near the flavin where three tyrosines align the substrate towards the N5–C4a region of the flavin (Figure 1). Mutational studies of these residues in MAO B[17] have shown that even though none of these residues is essential to catalysis, the affinity for and turnover of substrates is significantly altered in the mutants. For example, the K_m value for benzylamine increases by more than 10-fold in the Tyr435Phe mutant.[17] These residues also exert a dipole effect on the substrate that can make the amine more susceptible to oxidation.[17] Therefore, key features for substrate-positioning in the active site are proximity and orientation relative to the N5–C4a region of the flavin ring (Figure 1).

The notion and experimentally observed fact that **HIS** is not a physiological MAO substrate, whereas **NMH** is,[18] poses a very important and intriguing question: for a promiscuous enzyme such as MAO, what is the origin of its unexpected selectivity towards two very similar compounds, yet completely identical in their reactive ethylamino chain parts? The answer to this question might turn significant in designing novel and more efficient MAO inhibitors that are all in the clinical use as antidepressant and antiparkinsonian drugs,[6,19] while obtained results should suggest guidelines for the modification of the reactivity of these enzymes, providing achievements for the biotechnology and rational protein engineering. In the present study we used a combination of molecular dynamics (MD) simulations, MM-PBSA binding free energy calculations and quantum mechanical cluster approach to computationally address, for the first time in the literature, the substrate specificity of MAO B with two substrates, histamine (**HIS**) and *N*-methylhistamine (**NMH**), differing only in a single methyl group far away from the reactive centre.

Results and Discussion

Molecular Dynamics Simulations. Our analysis was initiated by examining the conformational flexibility of **HIS** and **NMH** molecules within the MAO B active site. For that purpose, classical MD simulations were performed and their stability was evaluated by analyzing the Root Mean Squared Deviation (RMSD) as a function of time, which measures how much the protein structure changes over the course of the simulation (Figure S1). The RMSDs for both substrates were not so much different from each other, and during the first 100 ns, RMSDs of all complexes were steadily increased as the enzyme deviated from its initial structure. After the initial 150 ns, the RMSD values cluster and remain in a narrow range around 2.5 Å, confirming the validity of the employed simulation times.

We monitored the orientation of substrates relative to the enzyme FAD co-factor with particular focus on the distance between the α–carbon on the substrate and the N5 atom on the

FAD co-factor (Figure 2) as these two sites represent the abstracting and accepting centres for the hydride transfer,[9,10,20] respectively, and their close vicinity assures substrate reactive conformation. Visual inspection of the evolution of these distances indicates that, for the **NMH** substrate, there is practically always a reactive conformation in either of the two MAO B subunits associated with αC(substrate)–N5(FAD) distances between 3–4 Å. This agrees with our earlier DFT calculated value of 3.198 Å in the Michaelis complex of dopamine within a cluster model of the MAO B enzyme,[9] and the results presented later. In contrast, simulations with the **HIS** substrate reveal that in one MAO B subunit a reactive conformation is even never achieved as, during the first 200 ns, all αC(substrate)–N5(FAD) distances are found well above 4 Å, and then start reaching values as high as 8–14 Å in the last 100 ns of simulations (Figure 2), which indicates substrate departure from the active site. These observations are further supported by the calculated average αC(substrate)–N5(FAD) distances during the whole 300 ns MD simulations, which are 4.994 and 6.224 Å for **NMH** in both enzyme subunits, while are increased to 5.820 and 7.243 Å for **HIS**. Taken all together, these results indicate that it is somewhat easier for **NMH** to achieve reactive conformations within the active site, which represents a small contribution towards the selectivity of MAO B for this substrate.

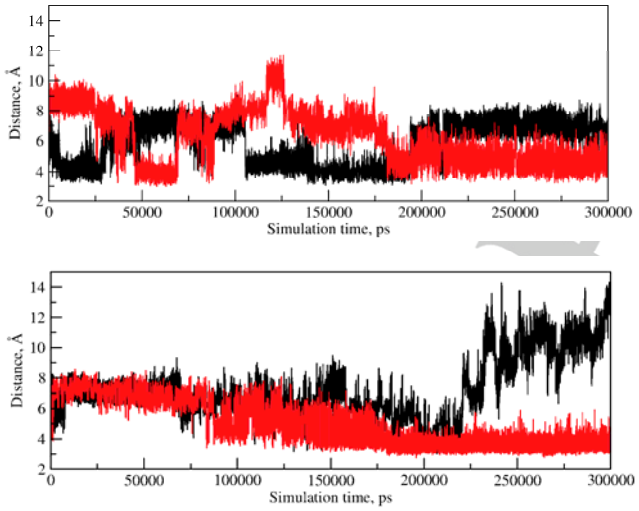

Figure 2. Evolution of the αC(substrate)–N5(FAD) distances during MD simulations for monocationic *N*-methylhistamine (top) and histamine (bottom) within the MAO B active site. The values corresponding to each of the enzyme subunits are indicated with red and black colours.

From these MD simulations, we identified three major reasons to why **NMH** is better anchored within the enzyme, thus better prepared for the catalytic step (representative structures are shown in Figure 3). Firstly, it appears that during simulations **NMH** prefers the *gauche* conformation in which there is an intramolecular hydrogen bond between its ethylamino group and the imidazole imino nitrogen (Scheme 2), while **HIS** is mostly found in the *trans* conformation, the latter being its most dominant physiological form.[21] This is evident upon inspecting the distances between the relevant ring imino- and chain amino nitrogen atoms (Figure S2), which give averages of 3.403 and 4.043 Å for **NMH** in both MAO B subunits, while are significantly higher at 4.490 and 4.745 Å for **HIS**, thus clearly indicating a larger preference for the intramolecular hydrogen bonding in **NMH**. Although, during MD simulations, the conformational preferences of substrate molecules are modulated by the protein binding pocket and the results may not necessarily reflect the preferences of the unbound systems, a possible explanation for this trend is offered by analyzing the corresponding pK_a values.

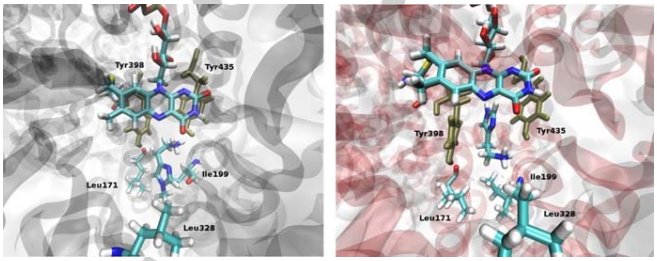

Figure 3. Representative structure of the most populated cluster of MAO B in complex with *N*-methylhistamine (left) and histamine (right) obtained after the clustering analysis of the corresponding MD trajectories. *N*-methylhistamine is properly positioned for the chemical reaction orienting its ethylamino group towards the N5 atom of the FAD co-factor.

Interestingly, while basicities of ring imino nitrogens in **NHM** and **HIS** are identical (both pK_a values reported at 5.8),[22] the basicity of the ethylamino group in **NMH** is slightly lower (pK_a = 9.57 vs. pK_a = 9.75 in **HIS**),[22] thus suggesting slightly higher acidity of the corresponding $-NH_3^+$ moiety in **NMH**. This implies that the cationic ethylamino group in **NMH** is somewhat more likely to form the intramolecular hydrogen bonding than in **HIS**, as it, for example, follows from the proposed *pK_a slide rule*.[23] This *gauche* conformation results in a more rigid and compact structure of **NMH**, which is less likely to move around the active site, and once it establishes a reactive conformation it remains in it for a longer time. In contrast, the preferred *trans* conformation of **HIS** makes it more flexible, thus allowing it to assume many orientations other the necessary reactive ones. Secondly, the imidazole ring in **HIS** has an acidic N–H group, permitting unreactive conformations to be achieved by its ability to form hydrogen bonds with active site residues, particularly interesting being those with the N5 atom and the near carbonyl group on the FAD co-factor (Figure 1). Since the former site is responsible for the C(α)–hydride abstraction, this hinders the **HIS** reactivity.

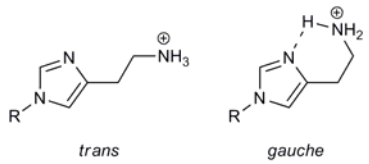

Scheme 2. Possible *trans* and *gauche* conformations of the monocationic histamine (**HIS**, R = H) and *N*-methylhistamine (**NMH**, R = Me).

Table 1. MM–PBSA calculated binding free energies (ΔG_{bind}) and their components[a] for the monocationic histamine (**HIS**) and *N*-methylhistamine (**NMH**) within the MAO B active site (in kcal mol^{-1}).

System	E_{VDW}	E_{elec}	E_{PB}	$E_{nonpolar}$	ΔH_{gas}	ΔH_{solv}	ΔH_{bind}	$T\Delta S$	ΔG_{bind}[b]	$\Delta G_{bind,EXP}$[c]	K_m[c,d]	k_{cat} / K_m[c,e]
HIS	–15.0	–139.1	144.7	–3.2	–154.1	141.5	–12.6	–15.3	2.8 ± 0.8	–3.3	~4000	0.875
NMH	–23.3	–131.4	136.6	–3.3	–154.7	133.3	–21.4	–15.8	–5.6 ± 0.5	–5.2	166 ± 8.1	210.8

[a] EVDW = van der Waals contribution from MM; Eelec = electrostatic energy calculated by the MM force field; EPB = electrostatic contribution to the solvation free energy calculated by PB; Enonpolar = nonpolar contribution to the solvation free energy calculated by empirical model. [b] Standard errors (SE) are calculated as SE = SD / √(sample size), where SD = standard deviation and sample size was 100 structures in our case. [c] Experimental results from Edmondson and co-workers.[11] [d] in μM. [e] in min^{-1} μM^{-1} × 1000.

The mentioned hydrogen bonds are further promoted by the stabilizing π–π stacking interactions of the **HIS** imidazole ring with the phenyl rings of the "aromatic cage" Tyr398 and Tyr435 (Figure 3), which all position the converting ethylamino group far from the enzyme co-factor and disable the catalysis. Thirdly, the substitution of the acidic imidazole N–H fragment in **HIS** with the N–Me group in **NMH** strongly favours hydrophobic interactions within the demonstrated hydrophobic nature of the MAO B active site[24] especially with the side chains of Leu171, Ile199 and Leu328 (Figure S3) that keep **NMH** anchored in the active site and properly oriented for the reaction. As expected, for around half of the simulation time, **HIS** makes no interactions with any of the three mentioned residues, while during the rest of simulations the number of interactions is mostly between 0 and 1. In contrast, **NMH** always forms hydrophobic contacts with at least one of those residues, and frequently with all three (Figure S3). It seems that particularly significant are interactions with Ile199, which was experimentally proposed as the "gating residue" in MAO B,[25,26] in some studies together with Tyr326.[27] Interestingly, Ile199 is conserved in all known MAO B sequences except bovine MAO B, which has Phe in this position that is, in turn, a conserved residue in the analogous position in MAO A. It is suggested that in a "closed conformation", Ile199 separates hydrophobic entrance- and substrate cavities in MAO B thus producing a bipartite configuration of the active site, while its "open conformation" allows the fusion of both cavities to a large total volume of ~700 Å^3, much larger than a monopartite substrate cavity of ~550 Å^3 in MAO A, and a successful substrate or inhibitor binding.[25,26] Conversion of Ile and Tyr gating side chains to Ala residues in MAO B resulted in no major structural alterations in the active site, but the double-mutated enzyme exhibits inhibitor-binding properties more similar to those of MAO A than to MAO B,[27] which together with the observation that Ile199Ala mutant show an increase in binding affinity for reversible MAO B inhibitors that bridge both cavities,[27] underlines a critical role of Ile199 in determining substrate and inhibitor binding specificity for MAO B. The results presented here provide further confirmation in this direction as this insight should prove valuable in the design of high affinity and specific reversible MAO B inhibitors.

In order to quantify these observations, we employed MM–PBSA analysis to estimate the absolute binding free energies for both **NMH** and **HIS** within the MAO B active site and to obtain detailed information about energetic contributions that govern these interactions (Table 1). Looking first at the overall binding free energies, our results clearly confirm that **NMH** is significantly better accommodated within MAO B as evidenced in a negative ΔG_{bind} value. This conclusion is strongly supported by a particularly impressive agreement between the calculated ΔG_{bind}(**NMH**) = –5.6 kcal mol^{-1} and the related experimental value of ΔG_{bind} = –5.2 kcal mol^{-1}, derived from the only available experimentally measured K_m(**NMH**) value of 166 ± 8.1 μM.[11] Although the matching quantitative agreement for **HIS** is only moderate, the results in Table 1 are very useful in indicating that intrinsic gas-phase binding enthalpies are practically the same for both substrates, so are the entropic contributions, which is sensible knowing the structural similarity among both substrates. Difference in the MAO B selectivity towards **NMH** and **HIS** originates from different enzyme solvation enthalpy term, ΔH_{solv}, which is much less-positive for **NMH**, thus leading to more exergonic and favourable binding. This suggests that MAO B is somewhat better preorganized to accommodate **NMH**, being fully in line with the observed stabilizing hydrophobic interactions reported for **NMH** here, in this way contributing to the MAO B selectivity. In ending this section, we note in passing that estimated errors of the MM–PBSA calculations shown in Table 1 are an order of magnitude lower than the discussed ΔG_{bind} values, offering some validity to the presented conclusions.

Although the focus of this work is on relative differences in the MAO B selectivity towards two very similar substrates, a somewhat significant mismatch between the calculated and experimentally derived ΔG_{bind} values for **HIS** deserves some comment. Given the complexity of computationally evaluating binding free energies of small molecules within large biological systems, and the known imperfections in the used state-of-the-art MM–PBSA approach,[28] a quantitative disagreement of 6.1 kcal mol^{-1} would, to some extent, even be acceptable for this kind of calculations. Still, this points to a conceptual difference, since the experimental value is negative ($\Delta G_{bind} < 0$), suggesting a favourable binding, while the computational value is positive ($\Delta G_{bind} > 0$), indicating an unlikely binding of **HIS** to the MAO B active site (Table 1). Even though the measured ΔG_{bind} for **NMH** is around 2 kcal mol^{-1} more exergonic, thus correctly implying a little competition between **NMH** and **HIS** for the MAO B binding when both substrates are present, the experimental ΔG_{bind}(**HIS**) = –3.3 kcal mol^{-1} would not help in explaining the experimental fact that **HIS** alone is not at all a physiological MAO B substrate, but has to be *N*-methylated before the enzymatic conversion.[18] While the value for **NMH** was precisely measured at K_m = 166 ± 8.1 μM,[11] Edmondson and co-workers experienced difficulties in

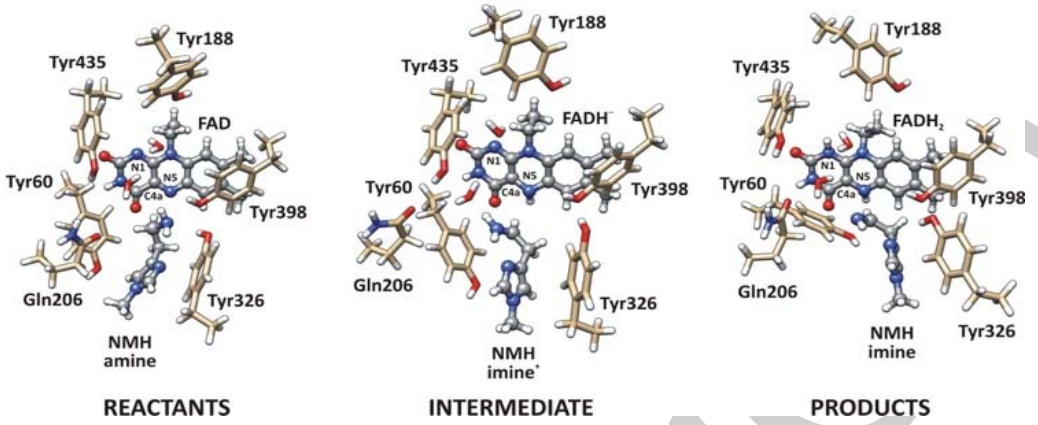

Figure 4. Structures of relevant stationary points for the MAO B catalyzed degradation of *N*-methylhistamine (**NMH**) within a cluster model of the enzyme. Geometries of the corresponding systems with histamine (**HIS**) are analogous.

measuring the *in vitro* K_m data for **HIS** and reported only an approximate value of K_m ~ 4000 μM,[11] which leads us to conclude that it is likely associated with some uncertainty and perhaps somewhat overestimating the binding. In addition, experimental K_m values[11] were not attained using the complex two substrate kinetics with both amine and oxygen,[29] which was shown by Ramsay and co-workers can give 1–2 kcal mol^{-1} variations in the K_m values for the oxidised and reduced forms of MAO B.[29] All of this sheds some concerns about a direct comparability among measured and computed ΔG_{bind}(**HIS**), and data reported here should primarily be regarded in terms of their interrelation, which indicates a trend that is strongly in line with experiments, and less from the viewpoint of the absolute agreement with experimental values. Taken all together, we feel that a more precise $\Delta G_{bind,EXP}$(**HIS**) should be closer to zero, or even slightly positive, which would then be more consistent with the fact that **HIS** is not at all metabolized by MAO B *in vivo*.[18]

Quantum Mechanical Analysis of the Catalytic Reaction. Following molecular dynamics simulations, we created a cluster model of the MAO B enzyme with both **HIS** and **NMH** substrates, including the FAD co-factor and Tyr60, Tyr188, Tyr326, Tyr398, Tyr435 and Gln206 residues, together with two active site water molecules, whose initial positions are analogous to those in the available MAO B crystal structure[25] and which we previously demonstrated are chemically involved in the catalysis.[9] M06–2X/6–31G(d) optimization gave the initial stationary points corresponding to Michaelis reactant complexes (Figure 4).

In reactants, both substrates are predominantly anchored through hydrogen bonds with Tyr326 and Tyr398, with the N(ring imino)–O(Tyr326) and N(chain amino)–O(Tyr398) distances at 2.783 and 3.326 Å for **HIS**, and slightly shorter at 2.730 and 3.015 Å for **NMH**, respectively. Even at this truncated model of the enzyme, these values indicate that **NMH** is somewhat better adjusted in the active site. Still, these pronounced interactions with the active site residues position the reacting α–CH fragment in **NMH** slightly further away from the flavin N5 atom, with the corresponding C(α)–N5 and H(α)–N5 distances at 3.452 and 2.933 Å, respectively, being shorter in **HIS** at 3.300 and 2.671 Å.

Direct substrate α–hydride abstraction turned out to be feasible in both substrates (Figure 5), in agreement with our previous results for dopamine[9,10] and noradrenaline[20] degradations. In the transition state, the transferring hydrogen is placed between the leaving α–carbon and the accepting flavin N5 atom, with bond distances at 1.419 and 1.225 Å for **HIS**, respectively, being slightly more symmetrical in **NMH** at 1.398 and 1.235 Å, in the same order. The free energy required for this process in **NMH** is 20.4 kcal mol^{-1} (ν_{imag} = 1414*i* cm^{-1}), which is increased to 23.0 kcal mol^{-1} in **HIS** (ν_{imag} = 1260*i* cm^{-1}), being in full agreement with the experimentally determined selectivity of MAO B towards these two substrates. The fact that this process is indeed associated with the transfer of a hydride anion (H^-) is evident in the calculated atomic charges (Table 2). Initially, total charges on **NMH** and the FAD co-factor in the reactants are 0.03 and –0.03 |e|, respectively, to be altered to 0.30 and –0.31 |e| in the transition state, respectively, thus indicating that during the reaction **NMH** loses around one third of an electron which is subsequently accommodated on FAD. In addition, the charge on

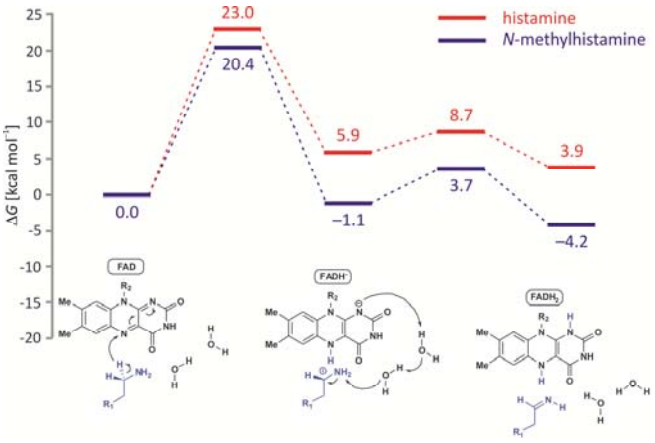

Figure 5. Free energy profiles for the MAO B catalyzed histamine (in red) and *N*-methylhistamine (in blue) degradation within a cluster model of the enzyme.

Table 2. Charge distribution during the rate-limiting hydride abstraction step in the MAO B catalysis as obtained through the NBO analysis at the (CPCM)/M06–2X/6–31G(d) level.

System	Atom/Molecule	Isolated	Reactants	TS	Products
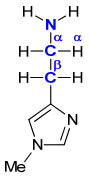	N(amino)	–0.94	–0.95	–0.80	–0.69
	α–H	0.23	0.24	0.33	0.43
	α–C	–0.26	–0.27	–0.07	0.27
	β–C	–0.51	–0.51	–0.52	–0.57
	***N*-methylhistamine**	0.00	0.03	0.30	0.84
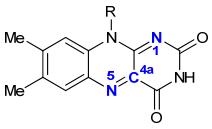	N5	–0.35	–0.36	–0.48	–0.67
	C4a	0.12	0.13	–0.06	–0.11
	N1	–0.67	–0.67	–0.71	–0.73
	FAD co-factor	0.00	–0.03	–0.31	–0.89

the accepting N5 atom changes from –0.36 in reactants to –0.48 |e| in the transition state. This agrees well with the electrophilic nature of the flavin N5 atom, which was revealed after we demonstrated that the irreversible MAO B inhibition by acetylenic inhibitors rasagiline, selegiline and clorgyline could proceed through the nucleophilic attack of the terminally deprotonated anionic inhibitor onto the flavin N5 atom,[30,31] the resulting complex matching the available X-ray structures.[15b,25,32] Interestingly, the charge on the substrate α–carbon atom, from which the H^- anion is abstracted, changes only moderately from 0.23 to 0.33 |e|, which is rationalized by the presence of the neighbouring amino group that stabilizes the formed carbocation through electron donation. This is seen in the reduced charge on the amino nitrogen and the shortened N(amino)–C(α) distance, changing from –0.95 |e| and 1.495 Å in the reactants to –0.80 |e| and 1.349 Å in the transition state, which is all consistent with the proposed H^- transfer.

It is particularly important to discuss the charge distribution in initial reactants in the context of the polar nucleophilic mechanism, which was proposed as another alternative for the amine oxidation involving proton (H^+) abstraction from the α–carbon as the rate-limiting step.[33] The crucial issue relating to this mechanism is what moiety on the enzyme would be a strong enough base to perform this task, since the reacting C–H group is poorly acidic with typical pK_a values as high as 25.[34] Structural analysis of both MAO isoforms shows there are no basic active-site residues that could act as proton acceptors.[35] Edmondson and co-workers upheld their arguments by stating that in MAOs the flavin co-factor is bent by around 30° from planarity about the N5–N10 axis, which enhances the basicity of the N5 atom and depletes the electron density on the C4a atom, thus facilitating substrate N(amino)–C4a(flavin) complex formation making subsequent proton abstraction possible,[35] although no direct evidence for a stable amine–flavin adduct has ever been found experimentally. We performed a relaxed-geometry scan of the mentioned N(amino)–C4a(flavin) bond, starting from 2.875 Å in the reactants with **NMH** and compressing it with 0.1 Å increments. The results showed no indications of the formation of a stable complex accompanied only by an increase in the total energy to values over 40 kcal mol^{-1} for the corresponding bond lengths shorter than 1.375 Å. In addition, NBO charges on the flavin C4a and N5 sites and the substrate N(amino) atom in the reactants are 0.13, −0.36, and −0.95 |e|, respectively, being practically unchanged from the values in isolated flavin and **NMH** (0.12, −0.35, and −0.94 |e|; Table 2), revealing there is no significant charge transfer in the Michaelis complex. On the other hand, based on QM/MM results on benzylamines, Kästner and co-workers showed that a formal hydride transfer could occur in a concerted asynchronous way involving the preceding transfer of two electrons from the amino group followed by the C(α)–H proton transfer,[36a] which they attributed in favour of the polar nucleophilic mechanism, though they also failed to provide any evidence for a stable amine–flavin adduct, which was proposed to facilitate deprotonation.[35] They claim that about 30−40% of the charge is transferred from the substrate to the co-factor already in the reactants,[36a] but later showed that this critically depends on the substrate–flavin orientation and polarization effects of the enzyme environment (MAO A vs. MAO B).[36b] In contrast, data in Table 2 clearly show that only 3% of the charge is perturbed upon substrate binding, which, taken all together, suggests that neutral amines do not exhibit the necessary nucleophilicity to readily add to the flavin C4a position. This all led us to rule out the polar nucleophilic mechanism as feasible, in agreement with our previous results,[9,10,37] and very recent experiments.[13] This is further supported by analyzing the flavin geometry in reactants, which is not bent, but practically planar with dihedral angles around N5–N10 axis of only 3.0 and 3.8° for **NMH**, and 0.8 and 1.0° for **HIS**.

Following the initial hydride transfer, the system relaxes to the corresponding intermediates, which are characterized by the formed semi-reduced anionic flavin, $FADH^-$, and the cationic substrate (Figures 4 and 5). This is indicated in the charge distribution, which shows that the full formation of the new N5–H^- bond increases the total charge on flavin to –0.89 |e|, while, accordingly, the charge on **NMH** becomes 0.84 |e|. The reaction with **NMH** is more favourable (ΔG_r = –1.1 kcal mol^{-1}), as the hydride abstraction in **HIS** is more endergonic (ΔG_r = 5.9 kcal mol^{-1}). It is important to emphasize that a significant difference

compared with dopamine degradation is the fact that, in the intermediate, there is no adduct formation between flavin and either **HIS** or **NMH** as it was demonstrated to occur with dopamine (Scheme 3), where the N5(flavin)–C(α) adduct was rather stable (ΔG_{form} = –27.7 kcal mol^{-1}) and formed spontaneously following the H$^-$ transfer.[9] There, the adduct decomposed concertedly with the substrate free amino group deprotonation during the next step in the MAO catalysis, facilitated by the availability of the acidic amino N–H bond. This is why the adduct formation rationalizes why many alkyl- and arylamines change from being MAO substrates to irreversible MAO inhibitors upon *N*,*N*-dimethylation,[38] making the adduct formation with dopamine fully justified.[9] With **HIS** and **NMH**, we observed no spontaneous adduct formation, which is not strikingly surprising since these two systems are chemically different from dopamine. Instead, cationic **NMH** and **HIS** are well separated from flavin in the matching intermediates (Figure 4) with the C(α)–N5(flavin) distances being 2.872 and 2.575 Å, respectively. Still, our calculations show that the adduct formation is possible, however it is associated with a free energy barrier (5.2 kcal mol^{-1} for **NMH** and 4.9 kcal mol^{-1} for **HIS**), while the corresponding adducts are less stable than the initial intermediates (2.5 kcal mol^{-1} for **NMH** and 3.1 kcal mol^{-1} for **HIS**). All of this led us to conclude that adduct found for dopamine is very unlikely to form with **NMH** and **HIS**, and that the subsequent substrate N–H deprotonation could occur without prior adduct formation.

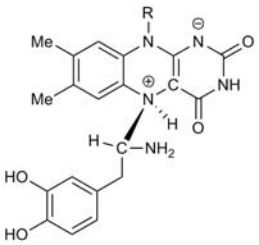

Scheme 3. Schematic representation of the covalent adduct that is spontaneously formed between dopamine and the flavin co-factor within the MAO B active site following the hydride transfer as outlined in ref. 9.

The next step in the amine degradation involves substrate amino group deprotonation by the flavin N1 atom to which it is connected with two active site waters through a network of hydrogen bonds (Figure 4). For example, in **NMH** the corresponding bond distances are N(**NMH**)–O(water1) = 2.690 Å, O(water1)–O(water2) = 2.733 Å, and O(water2)–N1 = 2.736 Å. This allows the amino N–H deprotonation assisted by the mentioned water molecules via the de Grotthuss mechanism.[39] This reaction is prompted by a negative charge build-up on the N1 atom following the hydride transfer (Table 2) and the fact that this site represents the most basic position within the co-factor moiety as demonstrated previously.[9] In **NMH**, this process is accompanied with the activation free energy of 4.8 kcal mol^{-1} (ν_{imag} = 792*i* cm^{-1}), which is slightly reduced in **HIS** to 2.8 kcal mol^{-1} (ν_{imag} = 834*i* cm^{-1}). This shows that the barrier for the substrate N–H deprotonation is much lower than that for the hydride abstraction in both cases, suggesting that the latter process represents the rate-limiting step of the overall transformation, being in full agreement with our earlier results[9,10,37] and recent experiments.[13] The low barrier of the second step is easily rationalized if one considers the corresponding pK_a values of the interacting sites. Namely, protonated imines are significantly more N–H acidic than neutral imines or amines, and are typically associated with pK_a ≈ 5–7,[34] which is well matched with the basicity of the N1 position in semi-reduced flavin FADH$^-$ that was experimentally estimated to be around pK_a ≈ 7,[40] thus the low barrier for the proton transfer. Upon deprotonation, the system gets stabilized by 4.8 kcal mol^{-1} in **HIS** and much significantly by 7.9 kcal mol^{-1} in **NMH**, which, in the latter, makes the whole reaction energetically feasible (Figure 5). In other words, the overall transformation in **NMH** is exergonic, ΔG_r = –4.2 kcal mol^{-1}, while in **HIS** it is endergonic, ΔG_r = 3.9 kcal mol^{-1}, thus making a significant contribution in rationalizing the selectivity of MAO B towards these substrates. In addition, the overall profile for **NMH** is favourable as it proceeds downhill in energy through stationary points at relative energies of 0.0, –1.1 and –4.2 kcal mol^{-1}, with the rate limiting hydride abstraction. The presented two-step process gives the neutral trans-imine and the fully reduced flavin as final products (Figure 4). The fact that flavin is fully reduced to $FADH_2$ enables an essential prerequisite for MAO regeneration by molecular oxygen, O_2, to revert flavin to its oxidized form, FAD, by producing hydrogen peroxide, H_2O_2, the reaction for which two hydrogen atoms are required. This gives a comparative advantage to our mechanistic picture in comparison with other proposals for MAO catalysis, which all advise flavin reduction to FADH$^-$ only.[33,37,38]

In finishing this section, it is very important to put the obtained activation free energies in the right perspective. At first sight, the calculated $\Delta G^{\ddagger}$(**NMH**) = 20.4 kcal mol^{-1} and $\Delta G^{\ddagger}$(**HIS**) = 23.0 kcal mol^{-1} appear off from experimental $\Delta G^{\ddagger}_{EXP}$(**NMH**) = 17.8 kcal mol^{-1} and $\Delta G^{\ddagger}$(**HIS**) = 19.2 kcal mol^{-1}, which are derived from the measured k_{cat}(**NMH**) = 35 min^{-1} and k_{cat}(**HIS**) = 3.5 min^{-1} values.[11] Still, it has to be emphasized that both of the calculated values are found well within the estimated error of the QM–cluster approach of 5 kcal mol^{-1}, assessed by Siegbahn and co-workers on the basis of extensive calculations for a large number of enzymes.[41] This approach uses a relatively small but well-chosen part of the enzyme, and it turned out very useful in revealing the feasibility of the direct hydride mechanism.[9,10,37] It is obvious that this computational methodology could be improved by either including a larger portion of the enzyme within this framework, or by considering the full dimensionality of the MAO B enzyme employing any of the established QM/MM techniques. To further refine the activation free energy, one could also proceed with the quantization of the hydrogen nuclear motion through path integral approaches[42a] or implicit schemes,[42b] giving rise to tunnelling,[43] which would additionally lower the barrier. The experimental value of the H/D kinetic isotope effect for MAO B is between 6–13,[33] suggesting significant tunnelling,[44] and giving additional evidence in support of the polar hydride transfer mechanism.[42a]

Nevertheless, the focus of this work was in rationalizing relative differences in the MAO B selectivity towards **HIS** and **NMH**, and, in that context, a very small difference in the experimental *in vitro* activation free energies of $\Delta\Delta G^{\ddagger}_{EXP}$ = 1.4 kcal mol^{-1} is very well reproduced by our calculations ($\Delta\Delta G^{\ddagger}_{CALC}$ = 2.6 kcal mol^{-1}). As a final point, we would like to reiterate that, following our earlier QM cluster results for dopamine,[9] the EVB QM/MM simulations brought the calculated barrier down from 24.4 kcal mol^{-1} to 16.1 kcal mol^{-1},[10] being in almost perfect agreement with experiments (16.5 kcal mol^{-1}),[11] thus supporting the hydride transfer mechanism. Therefore, we are confident that all conclusions regarding the MAO B selectivity consistently drawn from various computational techniques presented here are valid and convincing. Still, it remains a challenge to study the MAO catalysis with the **NMH** and **HIS** substrates through a combination of the QM/MM and path integral approaches, and although these are beyond the scope of the current manuscript, both aspects should bring calculated free energy barriers even closer to experiments and will be addressed in our future work.

Conclusions

In this work we used molecular dynamics simulations, MM–PBSA binding free energy evaluations, and quantum mechanical cluster calculations to investigate the specificity of the MAO B enzyme towards important neurotransmitter and signalling molecule histamine (**HIS**) and its *N*-methylhistamine derivative (**NMH**). Our results help in rationalizing the fact that **HIS** is not at all a physiological MAO B substrate, but has to be *N*-methylated to **NMH** before the enzymatic conversion, by showing that a dominant contribution for the MAO B selectivity is exerted in a 2.6 kcal mol^{-1} lower activation free energy for **NMH** for the rate-limiting hydride abstraction, in a very good agreement with the experimental value of $\Delta\Delta G^{\ddagger}_{EXP}$ = 1.4 kcal mol^{-1}.[11] For otherwise a very promiscuous enzyme, this unexpected and intriguing *in vivo* MAO B selectivity towards two substrates, identical in their reactive ethylamino fragments and differing only in a methyl group far from the reactive centre, is further promoted by several contributions. Firstly, **NMH** is less flexible within the active site due to its higher tendency to form rigid conformations with the intramolecular N(amino)–N(imino) hydrogen bonding, allowing **NMH** to spend more time in reactive orientations towards the flavin co-factor. On the other hand, **HIS** is less likely to form intramolecular hydrogen bonds and is more flexible, which often yields unreactive conformations that are additionally encouraged by the presence of the acidic N–H fragment on its imidazole ring permitting **HIS** to make unproductive hydrogen bonds with active site residues and the flavin co-factor itself. Secondly, the N–Me group on the imidazole ring in **NMH** favours its better binding through hydrophobic interactions with the side chains of Leu171, Leu328 and the "gating" Ile199 residue that all keep **NMH** anchored in the active site and properly oriented for the reaction. This is evident in the calculated MM–PBSA binding free energies, which predict more favourable binding for **NMH** (ΔG_{bind} = –5.6 kcal mol^{-1}) than for **HIS** (ΔG_{bind} = 2.8 kcal mol^{-1}), the former being in excellent agreement with the only available experimental value of –5.2 kcal mol^{-1}. Thirdly, the enzymatic transformation for both substrates follows our two-step hydride transfer mechanism, but the process is thermodynamically much more feasible for **NMH**, where the overall reaction free energy is exorgenic (ΔG_r = –4.2 kcal mol^{-1}), while for **HIS** it is endergonic (ΔG_r = 3.9 kcal mol^{-1}), thus unfavourable.

Our results provide the molecular interpretation and identification of structural determinants for the substrate specificity of the MAO B enzyme. The calculated free energy profiles are consistent with the hydride mechanism, where in the rate-limiting first step the flavin N5 atom abstracts the hydride anion from the substrate α–carbon, which is followed by the vicinal substrate N(amino)–H deprotonation by the flavin N1 atom assisted by two water molecules through de Grotthuss mechanism. In recent years, there have been several additional computational studies showing its prevailing energetic feasibility in MAO[12] or some other flavoenzymes,[45] together with a recent ^{13}C kinetic isotope effect measurements in a related polyamine oxidase flavoenzyme[13] that are strongly in line with the hydride transfer from the neutral amine. This study confirms the hydrophobic nature of the MAO B active site and underlines the important role of the Leu171, Leu328 and Ile199 residues in properly orienting substrates for the reaction. This insight might turn useful in rational modification of the MAO B reactivity in order to offer opportunities to exploit this enzyme in biotechnology and protein engineering, and in providing guidelines for designing more potent and selective MAO inhibitors that are all clinically employed in treating a variety of neuropsychiatric and neurodegenerative conditions.

Computational Section

Molecular dynamics simulations. The starting point for our calculations was the high-resolution (1.6 Å) X-ray structure of MAO B complexed with 2-(2-benzofuranyl)-2-imidazoline[25] obtained from the Protein Data Bank (accession code 2XFN). Original crystal waters were removed from the structure so that water molecules from the bulk solvent could diffuse into the active site during equilibration and production MD runs. The protein exists as a homodimer with covalently bound FAD co-factor to the conserved Cys397 residue in each subunit. Protonation states of ionisable residues were set according to PROPKA3.1 server predictions[46] and by inspecting hydrogen bonding networks in their closest vicinity, while the missing hydrogen atoms were added using the *tleap* module in AmberTools15.[47] For the FAD co-factor and both **HIS** and **NMH** substrates, geometry optimization and RESP charge calculations were performed with the Gaussian 09 program[48] at the HF/6–31G(d) level to be consistent with the employed GAFF force field, while the enzyme was modelled using the AMBER ff14SB force field. Since several experimental studies[49] and our previous computational results[24] have agreed in showing that MAO substrates are likely bound to the active site as monocations protonated at the chain amino group, which is usually the most abundant form of monoamines at physiological pH, we prepared two complexes involving monocationic **HIS** and **NMH** in their most stable N$^{\tau}$–H (N3–H) tautomeric forms[21a,50] each placed in both MAO B subunits. Thus formed protein complexes were solvated in a truncated octahedral box of TIP3P water molecules spanning a 10 Å thick buffer and submitted to geometry optimization in AMBER14 program.[47] Optimized systems were gradually heated from 0 to 300 K and equilibrated during 30 ps using NVT conditions followed by

productive and unconstrained MD simulations of 300 ns employing a time step of 2 fs at constant pressure (1 atm) and temperature (300 K), the latter held constant using Langevin thermostat with a collision frequency of 1 ps^{-1}. Bonds involving hydrogen atoms were constrained using the SHAKE algorithm,[51] while the long-range electrostatic interactions were calculated employing the Particle Mesh Ewald method.[52] The nonbonded interactions were truncated at 10.0 Å. Following MD simulations, the obtained structures were clustered according to the distance between the reactive αC(substrate)–N5(flavin) atoms on every 10th structure from the last 100 ns of simulations corresponding to the A subunit of the dimeric MAO B. Analogously, structures from the A subunit were also employed for all of the subsequent analyses here.

Free energy calculations. The binding free energy, ΔG_{bind}, of **HIS** and **NMH** within MAO B were calculated using the MM–PBSA protocol,[53] which is the widely used method for binding free energy calculations from the snapshots of MD trajectory[54] with an estimated standard error of 1–3 kcal mol^{-1}.[55] Within this approach, ΔG_{bind} is calculated as:

$$\Delta G_{bind} = < G_{complex} > - < G_{enzyme} > - < G_{substrate} > \quad (1)$$

where the symbol < > represents the average value over 100 snapshots collected from the 5 ns part of the corresponding MD trajectory where both substrates are equally oriented in reactive conformation in the active site. The free energy of a system can be approximated by three terms:

$$G_{complex/enzyme/substrate} = E_{MM} + G_{solv} - T \bullet \Delta S_{MM} \quad (2)$$

where E_{MM}, the gas-phase molecular mechanical energy, is obtained as a sum of $E_{internal}$, E_{VDW}, and E_{elec} contributions. G_{solv}, the solvation free energy, is a sum of polar (G_{polar}) and nonpolar ($G_{nonpolar}$) components, where the former was calculated by solving the finite-difference Generalized Born equation, while the latter was determined on the basis of the solvent-accessible surface area (SASA) as:

$$G_{nonpolar} = \gamma \bullet SASA + \beta \quad (3)$$

with recommended empirical parameters γ = 0.0054 kcal mol^{-1} $Å^{-2}$ and β = 0.92 kcal mol^{-1}.[56] The solute conformational entropy (SMM) was estimated by the normal-mode analysis based on 10 frames. The interior and exterior dielectric constants were set to 1 and 80, respectively.[57]

Quantum mechanical analysis. Following MD simulations, we selected a snapshot structure for each substrate from the part of the corresponding trajectory where the system assumed lowest energies while, at the same time, **HIS** and **NMH** were found in reactive conformations with their ethylamino chains pointing towards the FAD co-factor. This allowed us to build a cluster model of the MAO B enzyme by extracting initial positions of the substrate, FAD co-factor and Tyr60, Tyr188, Tyr326, Tyr398, Tyr435 and Gln206 residues, together with two active site water molecules whose positions were analogous to those of crystal structure waters HOH2329 and HOH2372, and which are, according to our previous calculations[9,37] in the right place to be chemically involved during catalysis. FAD co-factor was truncated at the ethyl group on the N10 atom, while all selected amino acids were truncated at their α-carbon atoms, which were kept in the form of the methyl group. All of the latter atom centres were used as anchor points and their positions were kept frozen during calculations. As mentioned, while MAO substrates are likely bound to the active site in their protonated forms, both experiments[49,58] and calculations[9,10,20,36] agree in indicating that the substrate neutral form is mandatory for the hydride abstraction. In the absence of basic residues in the active site,[35] substrate deprotonation before the enzymatic reaction could be achieved by several water molecules present in the enzyme. Hence, we striped one proton from each substrate and left them as neutral systems for the QM analysis. In order to minimize errors associated with the initial selection of starting geometries from MD trajectories, we tried several conformations of each substrate within the so-formed cluster and went on with the mechanistic calculations using the most stable complexes.

As a good compromise between accuracy and the computational feasibility, all geometries were optimized by the very efficient M06–2X/6–31G(d) method with thermal Gibbs free energy corrections extracted from the corresponding frequency calculations without the scaling factors. The final single-point energies were attained with a highly flexible 6–311++G(2df,2pd) basis set employing M06–2X, BMK, PBE0 and B3LYP DFT functionals. PBE0 offered results in closest agreement with experiments, and, together with the BMK and B3LYP results, provided barriers which are consistently lower than those with the M06–2X functional (Table S1), which is why PBE0 results are discussed throughout the text. In the applied cluster methodology, a truncated but carefully selected part of the enzyme is treated with the quantum mechanical methodology in accordance with our earlier work.[9,10,37] To account for polarization effects caused by the rest of the enzyme, we included, during both geometry optimization and single-point energy calculation, a conductor-like polarisable continuum model (CPCM)[59] with a common dielectric constant of ε = 4 and other parameters corresponding to pure water, as employed in many articles by Siegbahn, Himo and their co-workers in elucidating the catalytic mechanism of a large variety of enzymes.[60] This yields the (CPCM)/PBE0/6–311++G(2df,2pd)//(CPCM)/M06–2X/6–31G(d) model used here. Some validity to the choice of the cluster model to study enzyme catalysis is also provided through very recent papers by Warshel[61a] and Martínez[61b] and their co-workers, who demonstrated that in QM/MM approaches, which consider the full enzyme structure, the calculated activation barriers are not highly sensitive to the size of the QM region, beyond the immediate region that describes the reacting atoms. Hence, a reasonably large QM cluster employed here in conjunction with the implicit polarisable continuum representation of the rest of the enzyme should give reliable results. All of the transition state structures were verified to have the appropriate imaginary frequencies, from which the corresponding reactants and products were determined by the intrinsic reaction coordinate (IRC) procedure. Atomic charges were obtained by natural bond orbital (NBO)[62] analyses as the single-point calculations at the (CPCM)/M06–2X/6–31G(d) level of theory. All calculations were performed by using the Gaussian 09 software.[47]

Acknowledgements

A.M. wishes to thank the Croatian Science Foundation for a doctoral stipend through the Career Development Project for Young Researchers (contract number I–3376–2014). R.V. gratefully acknowledges the European Commission for an individual FP7 Marie Curie Career Integration Grant (contract number PCIG12–GA–2012–334493). We would like to thank the Zagreb University Computing Centre (SRCE) for granting computational resources on the ISABELLA cluster and the CRO–NGI infrastructure.

Keywords: histamine metabolism • histamine inactivation • monoamine oxidase selectivity • hydride transfer reaction • neurodegeneration and neuroprotective drugs

[1] C. Maslinski, W. A. Fogel In *Histamine and Histamine Antagonists*, (Ed.: B. Uvnäs), Springer: Berlin-Heidelberg, **1991**, pp. 165–189.

[2] H. G. Schwelberger, F. Ahrens, W. A. Fogel, F. Sánchez-Jiménez, In *Histamine H4 Receptor: a Novel Drug Target in Immunoregulatory and Inflammatory Diseases*, (Ed.: H. Stark), Versita: UK, **2013**, pp. 63–101.

[3] S. Chajkowski-Scarry, J. M. Rimoldi, *Fut. Med. Chem.* **2014**, *6*, 697–717.

[4] a) R. R. Ramsay, *Prog. Neuropsychopharmacol. Biol. Psychiatry* **2016**, *69*, 81–89; b) R. R. Ramsay, *R. Curr. Pharm. Des.* **2013**, *19*, 2529–2539; c) R. R. Ramsay, *Curr. Top. Med. Chem.* **2012**, *12*, 2189–2209.

[5] J. R. Miller, D. E. Edmondson, *J. Biol. Chem.* **1999**, *274*, 23515–23525.

[6] M. B. H. Youdim, D. E. Edmondson, K. F. Tipton, *Nat. Rev. Neurosci.* **2006**, *7*, 295–309.

[7] a) J. P. Klinman, *Acc. Chem. Res.* **2007**, *40*, 325–333; b) G. Gadda, *Biochemistry* **2012**, *51*, 2662–2669; c) D. E. Edmondson, *Curr. Pharm. Des.* **2014**, *20*, 155–160.

[8] M. Pavlin, M. Repič, R. Vianello, J. Mavri, *Mol. Neurobiol.* **2016**, *53*, 3400–3415.

[9] R. Vianello, M. Repič, J. Mavri, *Eur. J. Org. Chem.* **2012**, *2012*, 7057–7065.

[10] M. Repič, R. Vianello, M. Purg, F. Duarte, P. Bauer, S. C. L. Kamerlin, J. Mavri, *Proteins: Struct., Funct., Bioinf.* **2014**, *82*, 3347–3355.

[11] D. E. Edmondson, C. Binda, J. Wang, A. K. Upadhyay, A. Mattevi, *Biochemistry* **2009**, *48*, 4220–4230.

[12] a) M. A. Akyüz, S. S. Erdem, *J. Neural Transm.* **2013**, *120*, 937–945; b) V. E. Atalay, S. S. Erdem, *Comp. Biol. Chem.* **2013**, *47*, 181–191; c) G. Zapata-Torres, A. Fierro, G. Barriga-González, J. C. Salgado, C. Celis-Barros, *J. Chem. Inf. Model.* **2015**, *55*, 1349–1360.

[13] J. R. Tormos, M. B. Suarez, P. F. Fitzpatrick, *Arch. Biochem. Biophys.* **2016**, *612*, 115–119.

[14] a) M. Li, F. Hubálek, P. Newton-Vinson, D. E. Edmondson, *Protein Expr. Purif.* **2002**, *24*, 152–162; b) P. Newton-Vinson, F. Hubalek, D. E. Edmondson, *Protein Expr. Purif.* **2000**, *20*, 334–345.

[15] a) C. Binda, P. Newton-Vinson, F. Hubalek, D. E. Edmondson, A. Mattevi, *Nature Struct. Biol.* **2002**, *9*, 22–26; b) L. De Colibus, M. Li, C. Binda, A. Lustig, D. E. Edmondson, A. Mattevi, *Proc. Natl. Acad. Sci. U.S.A.* **2005**, *102*, 12684–12689.

[16] S. Y. Son, J. Ma, Y. Kondou, M. Yoshimura, E. Yamashita, T. Tsukihara, *Proc. Natl. Acad. Sci. U.S.A.* **2008**, *105*, 5739–5744.

[17] a) M. Li, C. Binda, A. Mattevi, D. E. Edmondson, *Biochemistry* **2006**, *45*, 4775–4784; b) M. A. Akyüz, S. S. Erdem, D. E. Edmondson, *J. Neural Transm.* **2007**, *114*, 693–698.

[18] a) E. F. Domino, *Schizophr. Bull.* **1980**, *6*, 292–297; b) J. D. Elsworth, V. Glover, M. Sandler, *Psychopharmacology* **1980**, *69*, 287–290.

[19] P. Riederer, L. Lachenmayer, G. Laux, *Curr. Med. Chem.* **2004**, *11*, 2033–2043.

[20] M. Poberžnik, M. Purg, M. Repič, J. Mavri, R. Vianello, *J. Phys. Chem. B* **2016**, *120*, 11419–11427.

[21] a) R. Vianello, J. Mavri, *New J. Chem.* **2012**, *36*, 954–962; b) J. Stare, J. Mavri, J. Grdadolnik, J. Zidar, Z. B. Maksić, R. Vianello, *J. Phys. Chem. B* **2011**, *115*, 5999–6010.

[22] D. D. Perrin, B. Dempsey, E. P. Serjeant in *pKa Prediction for Organic Acids and Bases*, Chapman and Hall: London, **1981**.

[23] P. Gilli, L. Pretto, V. Bertolasi, G. Gilli, *Acc. Chem. Res.* **2009**, *42*, 33–44.

[24] R. Borštnar, M. Repič, S. C. L. Kamerlin, R. Vianello, J. Mavri, *J. Chem. Theory Comput.* **2012**, *8*, 3864–3870.

[25] D. Bonivento, E. M. Milczek, G. R. McDonald, C. Binda, A. Holt, D. E. Edmondson, A. Mattevi, *J. Biol. Chem.* **2010**, *285*, 36849–36856.

[26] F. Hubálek, C. Binda, A. Khalil, M. Li, A. Mattevi, N. Castagnoli, D. E. Edmondson, *J. Biol. Chem.* **2005**, *280*, 15761–15766.

[27] E. M. Milczek, C. Binda, S. Rovida, A. Mattevi, D. E. Edmondson, *FEBS J.* **2011**, *278*, 4860–4869.

[28] a) G. Rastelli, A. Del Rio G. Degliesposti, M. Sgobba, *J. Comput. Chem.* **2010**, *31*, 797–810; b) T. Hou, J. Wang, Y. Li, W. Wang, *J. Chem. Inf. Model.* **2011**, *51*, 69–82.

[29] R. R. Ramsay, A. Olivieri, A. Holt, *J. Neural Transm.* **2011**, *118*, 1003–1019.

[30] M. Pavlin, J. Mavri, M. Repič, R. Vianello, *J. Neural Transm.* **2013**, *120*, 875–882.

[31] R. Borštnar, M. Repič, M. Kržan, J. Mavri, R. Vianello, *Eur. J. Org. Chem.* **2011**, 6419–6433.

[32] C. Binda, F. Hubalek, M. Li, Y. Herzig, J. Sterling, D. E. Edmondson, A. Mattevi, *J. Med. Chem.* **2005**, *48*, 8148–8154.

[33] J. R. Miller, D. E. Edmondson, *Biochemistry* **1999**, *38*, 13670–13683.

[34] M. Smith, J. March in *March's advanced organic chemistry: reactions, mechanisms and structure,* 5th ed., Wiley: New York, 2001.

[35] C. Binda, M. Li, F. Hubalek, N. Restelli, D. E. Edmondson, A. Mattevi, *Proc. Natl. Acad. Sci. U.S.A.* **2003**, *100*, 9750–9755.

[36] a) E. Abad, R. K. Zenn, J. Kästner, *J. Phys. Chem. B* **2013**, *117*, 14238–14246; b) R. K. Zenn, E. Abad, J. Kästner, *J. Phys. Chem. B* **2015**, *119*, 3678–3686.

[37] R. Vianello, C. Domene, J. Mavri, *Front. Neurosci*. **2016**, *10*, 327.

[38] C. Z. Ding, X. Lu, K. Nishimura, R. B. Silverman, *J. Med. Chem.* **1993**, *36*, 1711–1715.

[39] C. J. T. de Grotthuss, *Ann. Chim.* **1806**, *58*, 54–73.

[40] P. Macheroux, S. Ghisla, C. Sanner, H. Ruterjans, F. Muller, *BMC Biochem.* **2005**, *6*, 26–36.

[41] P. E. M. Siegbahn, T. Borowski, *Acc. Chem. Res.* **2006**, *39*, 729–738.

[42] a) J. Mavri, R. A. Matute, Z. T. Chu, R. Vianello, *J. Phys. Chem. B* **2016**, *120*, 3488−3492; b) M. Kržan, R. Vianello, A. Maršavelski, M. Repič, M. Zakšek, K. Kotnik, E. Fijan, J. Mavri, *PLoS One* **2016**, *11*, e0154002.

[43] D. R. Glowacki, J. N. Harvey, A. Mulholland, *J. Nature Chem.* **2012**, *4*, 169–176.

[44] T. Jonsson, D. E. Edmondson, J. P. Klinman, *Biochemistry* **1994**, *33*, 14871–14878.

[45] a) N. Gillet, J. J. Ruiz-Pernia, A. de la Lande, B. Levy, F. Lederer, I. Demachy, V. Moliner, *Phys. Chem. Chem. Phys.* **2016**, *18*, 15609–15618; b) B. Karasulu, W. Thiel, *ACS Catalysis* **2015**, *5*, 1227–1239; c) M. M. Kopacz, D. P. H. M. Heuts, M. W. Fraaije, *FEBS J.* **2014**, *281*, 4384–4393; d) Y. Cao, S. Han, L. Yu, H. Qian, J. Z. Chen, *J. Phys. Chem. B* **2014**, *118*, 5406–5417.

[46] M. H. M. Olsson, C. R. Søndergaard, M. Rostkowski, J. H. Jensen, *J. Chem. Theory Comput*. **2011**, *7*, 525– 537.

[47] D.A. Case, J.T. Berryman, R.M. Betz, D.S. Cerutti, T.E. Cheatham, III, T.A. Darden, R.E. Duke, T.J. Giese, H. Gohlke, A.W. Goetz, N. Homeyer, S. Izadi, P. Janowski, J. Kaus, A. Kovalenko, T.S. Lee, S. LeGrand, P. Li, T. Luchko, R. Luo, B. Madej, K.M. Merz, G. Monard, P. Needham, H. Nguyen, H.T. Nguyen, I. Omelyan, A. Onufriev, D.R. Roe, A. Roitberg, R. Salomon-Ferrer, C.L. Simmerling, W. Smith, J. Swails, R.C. Walker, J. Wang, R.M. Wolf, X. Wu, D.M. York and P.A. Kollman, AMBER 2015, University of California, San Francisco, **2015**.

[48] M. J. Frisch, G. W. Trucks, H. B. Schlegel, G. E. Scuseria, M. A. Robb, J. R. Cheeseman, G. Scalmani, V. Barone, B. Mennucci, G. A. Petersson, H. Nakatsuji, M. Caricato, X. Li, H. P. Hratchian, A. F. Izmaylov, J. Bloino, G. Zheng, J. L. Sonnenberg, M. Hada, M. Ehara, K. Toyota, R. Fukuda, J. Hasegawa, M. Ishida, T. Nakajima, Y. Honda, O. Kitao, H. Nakai, T. Vreven, J. A. Montgomery, Jr., J. E. Peralta, F. Ogliaro, M. Bearpark, J. J. Heyd, E. Brothers, K. N. Kudin, V. N. Staroverov, R. Kobayashi, J. Normand, K. Raghavachari, A. Rendell, J. C. Burant, S. S. Iyengar, J. Tomasi, M. Cossi, N. Rega, J. M. Millam, M. Klene, J. E. Knox, J. B. Cross, V. Bakken, C. Adamo, J. Jaramillo, R. Gomperts, R. E. Stratmann, O. Yazyev, A. J. Austin, R. Cammi, C. Pomelli, J. W. Ochterski, R. L. Martin, K. Morokuma, V. G. Zakrzewski, G. A. Voth, P. Salvador, J. J. Dannenberg, S. Dapprich, A. D. Daniels, Ö. Farkas, J. B. Foresman, J. V. Ortiz, J. Cioslowski, and D. J. Fox, Gaussian 09, Revision A.02; Gaussian, Inc., Wallingford, CT, **2009**.

[49] a) T. Z. Jones, D. Balsa, M. Unzeta, R. R. Ramsay, *J. Neural Transm.* **2007**, *114*, 707–712; R. V. Dunn, K. R. Marshall, A. W. Munro, N. S. Scrutton, *FEBS J.* **2008**, *275*, 3850–3858.
[50] G. A. Worth, W. G. Richards, *J. Am. Chem. Soc.* **1994**, *116*, 239–250.
[51] J. P. Ryckaert, G. Ciccotti, H. J. Berendsen, *J. Comput. Phys.* **1977**, *23*, 327−341.
[52] T. Darden, D. York, L. Pedersen, *J. Chem. Phys.* **1993**, *98*, 10089−10092.
[53] B. R. III Miller, D. Jr McGee, J. M. Swails, N. Homeyer, H. Gohlke, A. E. Roitberg, *J. Chem. Theory Comput.* **2012**, *8*, 3314–3321.
[54] G. G. Ferenczy In *Thermodynamics and Kinetics of Drug Binding*, (Eds.: G. M. Keserü, D. C. Swinney), Wiley: Weinheim, **2015**, pp. 37–61.
[55] A. Weis, K. Katebzadeh, P. Söderhjelm, I. Nilsson, U. Ryde, *J. Med. Chem.* **2006**, *49*, 6596–6606.
[56] P. A. Kollman, I. Massova, C. Reyes, B. Kuhn, S. Huo, L. Chong, M. Lee, T. Lee, Y. Duan, W. Wang, O. Donini, P. Cieplak, J. Srinivasan, D. A. Case, T. E. Cheatham, *Acc. Chem. Res.* **2000**, *33*, 889–897.
[57] D. Bashford, D. A. Case, *Annu. Rev. Phys. Chem.* **2000**, *51*, 129–152.
[58] A. K. Tan, R. R. Ramsay, *Biochemistry* **1993**, *32*, 2137–2143.
[59] M. Cossi, N. Rega, G. Scalmani, V. Barone, *J. Comput. Chem.* **2003**, *24*, 669–681.
[60] a) G. C. Patton, P. Stenmark, D. R. Gollapalli, R. Sevastik, P. Kursula, S. Flodin, H. Schuler, C. T. Swales, H. Eklund, F. Himo, P. Nordlund, L. Hedstrom, *Nat. Chem. Biol.* **2011**, *7*, 950–958; b) P. E. M. Siegbahn, F. Himo, *WIREs Comput. Mol. Sci.* **2011**, *1*, 323–336.
[61] a) G. Jindal, A. Warshel, *J. Phys. Chem. B* **2016**, *120*, 9913–9921; b) H. J. Kulik, J. Zhang, J. P. Klinman, T. J. Martínez, *J. Phys. Chem. B* **2016**, *120*, 11381–11394.
[62] J. P. Foster, F. Weinhold, *J. Am. Chem. Soc.* **1980**, *102*, 7211–7218.

Entry for the Table of Contents

FULL PAPER

A methyl game changer: Placed on the imidazole ring distant from the reactive ehylamino group, a single methyl group determines the preference of, otherwise highly promiscuous, monoamine oxidase enzyme towards physiologically important neurotransmitter histamine and its *N*-methyl derivative. A combination of MD simulations, MM–PBSA binding free-energy evaluations and QM calculations addresses this unexpected yet challenging selectivity.

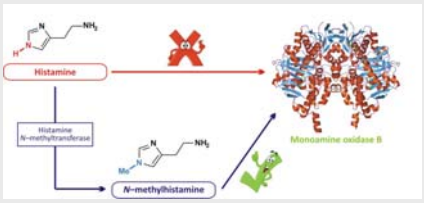

*Aleksandra Maršavelski, Robert Vianello**

Page No. – Page No.

What a difference a methyl group makes – the selectivity of monoamine oxidase B towards histamine and *N*-methylhistamine